Closed-loop cavitation control for focused ultrasound-mediated blood-brain-barrier opening by long-circulating microbubbles

Cavusoglu, Mustafa ; Zhang, Jia ; Ielacqua, Giovanna Diletta ; Pellegrini, Giovanni ; Signorell, Rea Deborah ; Papachristodoulou, Alexandros ; Brambilla, Davide ; Roth, Patrick ; Weller, Michael ; Rudin, Markus ; Martin, Ernst ; Leroux, Jean Christophe ; Werner, Beat

Abstract: Focused ultrasound (FUS) exposure in the presence of microbubbles (MBs) has been successfully used in the delivery of various sizes of therapeutic molecules across the blood-brain barrier (BBB). While acoustic pressure is correlated with the BBB opening size, real-time control of BBB opening to avoid vascular and neural damage is still a challenge. This arises mainly from the variability of FUS-MB interactions due to the variations of animal-specific metabolic environment and specific experimental setup. In this study, we demonstrate a closed-loop cavitation control framework to induce BBB opening for delivering large therapeutic molecules without causing macro tissue damages. To this end, we performed in mice long-term (5 min) cavitation monitoring facilitated by using long-circulating MBs. Monitoring the long-term temporal kinetics of the MBs under varying level of FUS pressure allowed to identify in-situ, animal specific activity regimes forming a pressure-dependent activity bands. This enables to determine the boundaries of each activity band (i.e. steady oscillation, transition, inertial cavitation) independent from the physical and physiological dynamics of the experiment. However, such a calibration approach is time consuming and to speed up characterization of the in-situ, animal specific FUS-MB dynamics, we tested a novel method called "pre-calibration" that closely reproduces the results of long-term monitoring but with a much shorter duration. Once the activity bands are determined from the pre-calibration method, an operation band can be selected around the desired cavitation dose. To drive cavitation in the selected operation band, we developed an adaptive, closed-loop controller that updates the acoustic pressure between each sonication based on measured cavitation dose. Finally, we quantitatively assessed the safety of different activity bands and validated the proposed methods and controller framework. The proposed framework serves to optimize the FUS pressure instantly to maintain the targeted

DOI: https://doi.org/10.1088/1361-6560/aafaa5

ultrasound-mediated blood-brain-barrier opening by long-circulating microbubbles. Physics in Medicine and Biology, 64(4):045012.
DOI: https://doi.org/10.1088/1361-6560/aafaa5

Closed-loop cavitation control for focused ultrasound-mediated blood-brain-barrier opening by long-circulating microbubbles

Closed-Loop Cavitation Control for Focused Ultrasound-Mediated Blood-Brain Barrier Opening by Long-Circulating Microbubbles

Mustafa Çavuşoğlu[1,2], Jia Zhang[2], Giovanna Diletta Ielacqua [2], Giovanni Pellegrini[3], Rea Deborah Signorell[4], Alexandros Papachristodoulou[5], Davide Brambilla[4,6], Patrick Roth[5], Michael Weller[5], Markus Rudin[2], Ernst Martin[1], Jean-Christophe Leroux[4], Beat Werner[1]

[1] Center for MR-Research, University Children's Hospital Zurich, 8032 Zurich, Switzerland

[2] Institute for Biomedical Engineering, ETH Zurich, 8091 Zurich, Switzerland

[3] Institute of Veterinary Pathology, University Hospital Zurich and University of Zurich, 8057 Zurich, Switzerland

[4] Institute of Pharmaceutical Sciences, Department of Chemistry and Applied Biosciences, ETH Zurich, 8093 Zurich, Switzerland

[5] Laboratory for Molecular Neuro-Oncology, University Hospital Zurich and University of Zurich, 8091 Zurich, Switzerland

[6] Faculty of Pharmacy, Université de Montréal, Quebec, Canada

Correspondence:

Dr. Mustafa Çavuşoğlu

ETH Zurich, Swiss Federal Institute of Technology

Information Technology and Electrical Engineering Dept.

Institute for Biomedical Engineering, ETZ F 64.1

Gloriastrasse 35, 8092, Zurich

Email: cavusoglu@biomed.ee.ethz.ch

Tel: +41 44 6324563

Abstract

Focused ultrasound (FUS) exposure in the presence of microbubbles (MBs) has been successfully used in the delivery of various sizes of therapeutic molecules across the blood-brain barrier (BBB). While acoustic pressure is correlated with the BBB opening size, real-time control of BBB opening to avoid vascular and neural damage is still a challenge. This arises mainly from the variability of FUS-MB interactions due to the variations of animal-specific metabolic environment and specific experimental setup. In this study, we demonstrate a closed-loop cavitation control framework to induce BBB opening for delivering large therapeutic molecules without causing macro tissue damages. To this end, we performed in mice long-term (5 min) cavitation monitoring facilitated by using long-circulating MBs. Monitoring the long-term temporal kinetics of the MBs under varying level of FUS pressure allowed to identify in-situ, animal specific activity regimes forming a pressure-dependent activity bands. This enables to determine the boundaries of each activity band (i.e. steady oscillation, transition, inertial cavitation) independent from the physical and physiological dynamics of the experiment. However, such a calibration approach is time consuming and to speed up characterization of the in-situ, animal specific FUS-MB dynamics, we tested a novel method called “pre-calibration” that closely reproduces the results of long-term monitoring but with a much shorter duration. Once the activity bands are determined from the pre-calibration method, an operation band can be selected around the desired cavitation dose. To drive cavitation in the selected operation band, we developed an adaptive, closed-loop controller that updates the acoustic pressure between each sonication based on measured cavitation dose. Finally, we quantitatively assessed the safety of different activity bands and validated the proposed methods and controller framework. The proposed framework serves to optimize the FUS pressure instantly to maintain the targeted cavitation level while improving safety control.

Introduction

Focused ultrasound (FUS) in combination with intravenously administered microbubbles (MBs) is a unique method to open the blood-brain barrier (BBB) locally, transiently and noninvasively (Hynynen *et al.*, 2001; McDannold *et al.*, 2005) . Using this technique, a variety of drugs with different sizes has been delivered to the brain parenchyma such as small anti-cancer chemotherapeutics (MW < 1000 Da)(Treat *et al.*, 2012), neurotrophins (MW ~20 kDa) (Baseri *et al.*, 2012), large amyloid β antibodies (MW ~150 kDa) (Jordao *et al.*, 2013) and other therapeutic macromolecules for treatment of glioblastoma (Liu *et al.*, 2010; Kovacs *et al.*, 2014), central nervous system (CNS) diseases (Timbie *et al.*, 2015). Following successful pre-clinical studies in a wide range of *in vivo* models including rodents, mammalians and non-human primates (NHP) (Marquet *et al.*, 2011; Wu *et al.*, 2016), FUS-based targeted drug delivery is currently evaluated in clinical trials for the treatment of malignant brain tumors invasively (Carpentier *et al.*, 2016) and Alzheimer's disease (Lipsman *et al.*, 2018).

The delivery rate of drug molecules is limited by the FUS-induced BBB opening size (Choi *et al.*, 2010; Marty *et al.*, 2012). The latter is linked to and controllable by modulating the applied acoustic FUS pressure (Chen and Konofagou, 2014). Furthermore, the size dependent trans-BBB delivery rate of drug molecules is correlated with FUS-induced cavitation activity. Depending on the level of acoustic pressure, microbubble activity is described as stable cavitation (SC, low-pressure, low-amplitude bubble oscillation) and inertial cavitation (IC, high-pressure, transient bubble collapse) (Neppiras, 1984; Miller *et al.*, 1996).

Passive cavitation detection (PCD) was proposed for real-time transcranial monitoring of the bubble behavior and resulting cavitation activity during FUS sonication (McDannold *et al.*, 2006). Recently, PCD- based cavitation metrics have been utilized to predict the cavitation dose and BBB opening size (Tung *et al.*, 2011), delivery efficiency of the molecules (Wu *et al.*, 2016) and permeability and reversibility of BBB opening (Sun *et al.*, 2015). It has been shown that FUS induced BBB opening does not necessarily require the occurrence of inertial cavitation. SC alone can provide a significant enhancement in the delivery efficiency of relatively large molecules (3-70 kDa) (McDannold *et al.*, 2006; Sun *et al.*, 2017). However, IC is needed to achieve delivery of very large molecules (500-2000 kDa) (Chen and Konofagou, 2014).

However, presence of IC increases the likelihood of vascular and neuronal damage as a result of violent bubble collapse (Aryal *et al.*, 2014).

Several previous publications attempted to achieve safe BBB opening by defining global values for the FUS pressures corresponding to thresholds for BBB opening, SC and IC. Tung *et al* reported pressures such as 0.30 MPa for BBB opening and 0.45 MPa for IC in mice using a 1.5 MHz FUS transducer (Tung *et al.*, 2010b). O'Reilly *et al* proposed an open-loop feed-back control to adjust the driving voltage of a FUS transducer operating at 551.5 kHz where the detection of ultra-harmonic emission from PCD signal is assumed to be the upper threshold for SC (O'Reilly and Hynynen, 2012). The pressure value was then set to a fraction of the determined threshold and the following sonication was performed at this fixed power level that was not further adjusted (open-loop). The pressure ranges for safe BBB opening from 0.18 MPa to 0.40 MPa. Tsai *et al* proposed to use energy spectral density (ESD) as a spectrogram-based metric and defined a BBB opening threshold on ESD as 5.5 dB for four different pressure levels using a 55 MHz FUS transducer (Tsai *et al.*, 2016). However, they found significant variation on the resulting ESD values and further reported that the necessary exposure time to open the BBB depends on the individual animal conditions even with an identical exposure level.

Modulating FUS pressure to compensate for inter-experimental discrepancies is still a major challenge. This mainly arises because designing such a real-time FUS power controller requires first to determine animal specific cavitation thresholds in-situ. Once the cavitation thresholds are defined, then the experiment can be executed in safe 'operation bands'. Obviously, determining global boundaries defining the limits of specific activity regimes independent from the physical (i.e. experimental setup, geometry, acoustic coupling) and physiological (i.e. inter-animal variation, physiological condition) dynamics of the experiment is not feasible. Additional difficulties in controlling cavitation activity arise from the varying concentration of the MBs over time after injection (Sun *et al.*, 2017). The decreased MB lifetime (30-60s) of commonly used MBs by long-burst exposure of FUS prevents to reveal a robust characterization of the dynamic FUS-microbubble interaction (Pouliopoulos *et al.*, 2014; Pouliopoulos *et al.*, 2016). Moreover, it has been reported that the targeted tissue type (i.e. gray and white matter) and vascular structure in the targeted volume may significantly influence the ultimate cavitation activity (Wu *et al.*, 2016).

In this work, we developed and validated a closed-loop, real-time cavitation control framework to maximize BBB opening without causing macro tissue damage. To achieve this, we first analyzed the 'long-term' (5 min) temporal dynamics of the FUS-MB interaction for a wide range of acoustic pressure levels. The ability of such a long-term PCD monitoring was facilitated by the utilization of long-circulating MBs. The long-term kinetic characterization enables to identify in-situ pressure dependent 'band structures' for different activity regimes. However, this is a highly time consuming task because the long-term PCD monitoring has to be repeated for a wide range of FUS-pressure levels. To overcome this, we tested a novel 'pre-calibration' method for fast determination of the desired operation band. For executing sonications reliably within this band, we developed an adaptive, closed-loop, feed-back power controller that dynamically updates FUS power between sonications. To assess the safety of the proposed methods, we quantified the severity of the tissue damage using a hemorrhage-scoring scheme. The controller setup subsequently was applied successfully in a preclinical study in mouse models of Glioblastoma Multiforme to deliver 80nm-sized liposomal MGMT inactivators (Signorell *et al.*, 2018) to reverse chemoresistance against temozolomide (Papachristodoulou et al., 2018).

Methods

Animal Preparation

All animal experimental procedures were reviewed and approved by the Cantonal Veterinary Office Zürich (Licence number 085/2014). A total of 35 wild-type adult female mice (strain: C57BL/6, age: 10 to 12 weeks, 25-28 g, Charles River, Freiburg, Germany) were used. Animals were anesthetized with 2-3% Isoflurane vaporized in a mixture of oxygen (flow rate: 1 L min-1 at 1.0 Bar, 21 °C). To maintain the body temperature, animals were placed on a heating pad with a stable temperature of ~ 38°C. The fur on the head was removed by using an electrical trimmer and a depilatory cream while the scalp and skull remained intact. A 27-gauge catheter was inserted into the tail vein for i.v. injections.

Experimental Setup

A schematic illustration of the setup for animal experiments is shown in figure.1. A MR-compatible six channel annular array transducer (center frequency: 650 KHz, external diameter: 30 mm, focal depth: 30 mm, Imasonic, Besancon, France) was used for sonication. The multi-element design allowed electronic steering of the ultrasound

beam in depth. The transducer was mounted on an MR-compatible rodent FUS system that provided computer control for parametrization of the sonications and a motorized positioning system (Image Guided Therapy, Pessac, France) (Magnin R, 2015). The transducer was acoustically coupled to the rodent head with a custom-built truncated cone filled with deionized and degassed water and closed with a thin latex membrane. The cone was positioned above the target volume under MR-imaging guidance. A spherically focused, polyvinylidene fluoride (PVDF) hydrophone (center frequency: 2 ± 0.2 MHz, Imasonic, Besancon, France) served as a passive cavitation detector for real-time monitoring of the acoustic emissions arising from MB cavitation. The hydrophone was coaxially aligned with the FUS transducer. A custom-built MATLAB (Mathworks, MA, USA) program was used to control the sonications through the systems controller and to analyze the acquired PCD signals. The PCD signal was amplified by 20 dB (AH-1100, Onda, CA, USA). The first (650 KHz) and second (1.3MHz) harmonic frequency components of the PCD signal was high-pass filtered (EF509, Thorlabs, NJ, USA) and digitized with 8 bit resolution using an USB driven oscilloscope (3204A, Pico Technology, Cambridgeshire, United Kingdom) at a sampling rate of 50 MHz.

BG8235 MBs, a non-commercial MB provided by Bracco Suisse SA, Geneva, Switzerland were used in this study. BG8235 is a phospholipid MB containing perfluorobutane with a mean-diameter of 3.24 μm and long circulating times similar to (Schneider *et al.*, 2011). The MBs were freshly diluted to 3 mL with normal saline solution and injected through the tail vein (0.01 μL/g) by using an automated syringe pump (Harvard Apparatus, Boston, MA, USA). The infusion rate was 1 μL/s. The sonication was started thirty seconds after the onset of the microbubble infusion. At the beginning of the FUS exposure, a control sonication without MB injection was performed to obtain a baseline for cavitation monitoring for 30 s (Arvanitis *et al.*, 2012).

Acoustic Cavitation Emission Quantification

As previously described (Tung *et al.*, 2010b; Wu *et al.*, 2014), acoustic emissions due to the MB-FUS interaction were quantified using inertial cavitation dose (ICD). Spectrograms were calculated for each acoustic emission signal acquired by the focused hydrophone. The harmonic $(nf, n = 1,2, \dots)$, sub-harmonic $(f/2)$ and ultra-harmonic $(nf/2,\ n = 3,5, \dots)$ frequencies were filtered by excluding ±150 kHz bandwidths to retain only the broadband response. The root-mean-square (rms) of the filtered spectral amplitude was computed to represent the ICD.

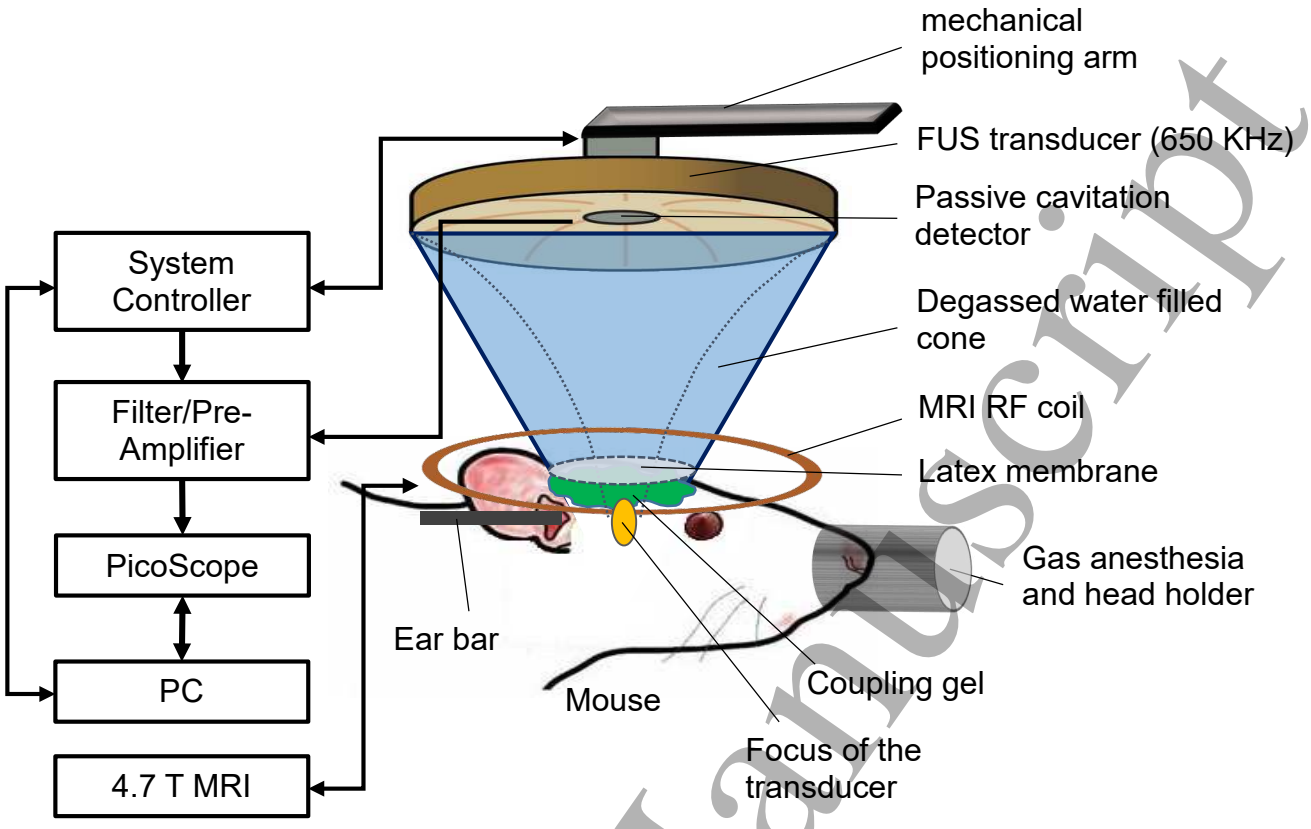

Figure 1. Schematic illustration of the experimental setup. A 650- kHz six channel MR-compatible focused ultrasound (FUS) transducer was used for sonication. It was confocally aligned with a spherically focused hydrophone for passive cavitation detection (PCD). The transducer and motorized 2-axis mechanical positioning arm were driven by the system controller. A cone filled with degassed and deionized water filled provided acoustic coupling between the transducer and the rodent head.

Long-Term ICD Monitoring

To explore the dynamics of the ICD over time, ICD values were monitored for 5 min ("long term") for a discrete range of acoustic pressure levels varying from 0.18 MPa up to 0.62 MPa with a step size of 0.03 MPa increments. For this purpose, seven mice were included in this part of the experiments. Figure.2.a illustrates the sonication scheme for long-term ICD monitoring. Following the injection of 50 µL of MBs, two consecutive pressure levels [0.25 MPa, 0.28 MPa] were repeatedly applied (pulse duration=10 ms, PRF=1 Hz) for 5 minutes duration and the ICD signal is monitored. A pre-pulse of 0.18 MPa was applied 5.6 ms before the onset of each sonication to obtain a reference baseline pressure level. Following the initial 5 min of recording, a fresh amount of 50 µL of MBs were injected and a second pair of acoustic pressure levels [0.31 MPa, 0.34 MPa] were repeatedly applied for 5 minutes duration and the ICD

signal is monitored. This procedure is repeated until the targeted acoustic pressure range is covered. Because two consecutive acoustic pressure levels were monitored following a fresh MB injection, the time that it takes to cover a range of acoustic pressures $[P_1, P_{2,\dots,} P_N]$ is $Nx5/2$ minutes. Third-degree polynomial curve fitting was applied to the acquired ICD data to obtain the long-term ICD kinetic curves.

Pre-Calibration Method

To apply in-*situ* pre-calibration in actual treatments, a sonication scheme was designed to scan the same range of pressure levels as in the long-term ICD monitoring experiments in much shorter amount of total time. It applies very short sonications (pulse duration=200 μs, PRF = 1 Hz) where 0.18 MPa pressure was emitted 5.6 ms before the onset of each pressure sequence as a low pressure baseline as in the long-term monitoring experiments (figure.2.b). This allows to acquire all pre-calibration curves with only a single 50 μL microbubble solution injection. Following the MB injection, the targeted acoustic pressure range $[P_1, P_N]$ is sonicated with an acoustic pulse series of $[P_1, P_{2,\dots,} P_N]$ in an increasing manner which takes N seconds. To be able to acquire enough data to ensure a robust curve fitting, the experiment is repeated R=10 times yielding a total duration of NxR seconds.

Closed-Loop Real-Time Feedback Power Control

A closed-loop real-time feedback power controller was developed to ensure execution of the treatment within the prescribed operation band. As before, the system relies on the real-time acquisition of the PCD signal, calculation of the instant ICD from the acoustic spectrogram of the acquired PCD signal, comparison of the instant ICD with the pre-determined boundaries of the operation band and determining the optimum FUS power to be applied for the next sonication. The controller decides for the optimum power level for the next time point by assessing the history in a certain time window (i.e. 10 s) instead of a single time point. The controller algorithm is described in detail in the appendix.

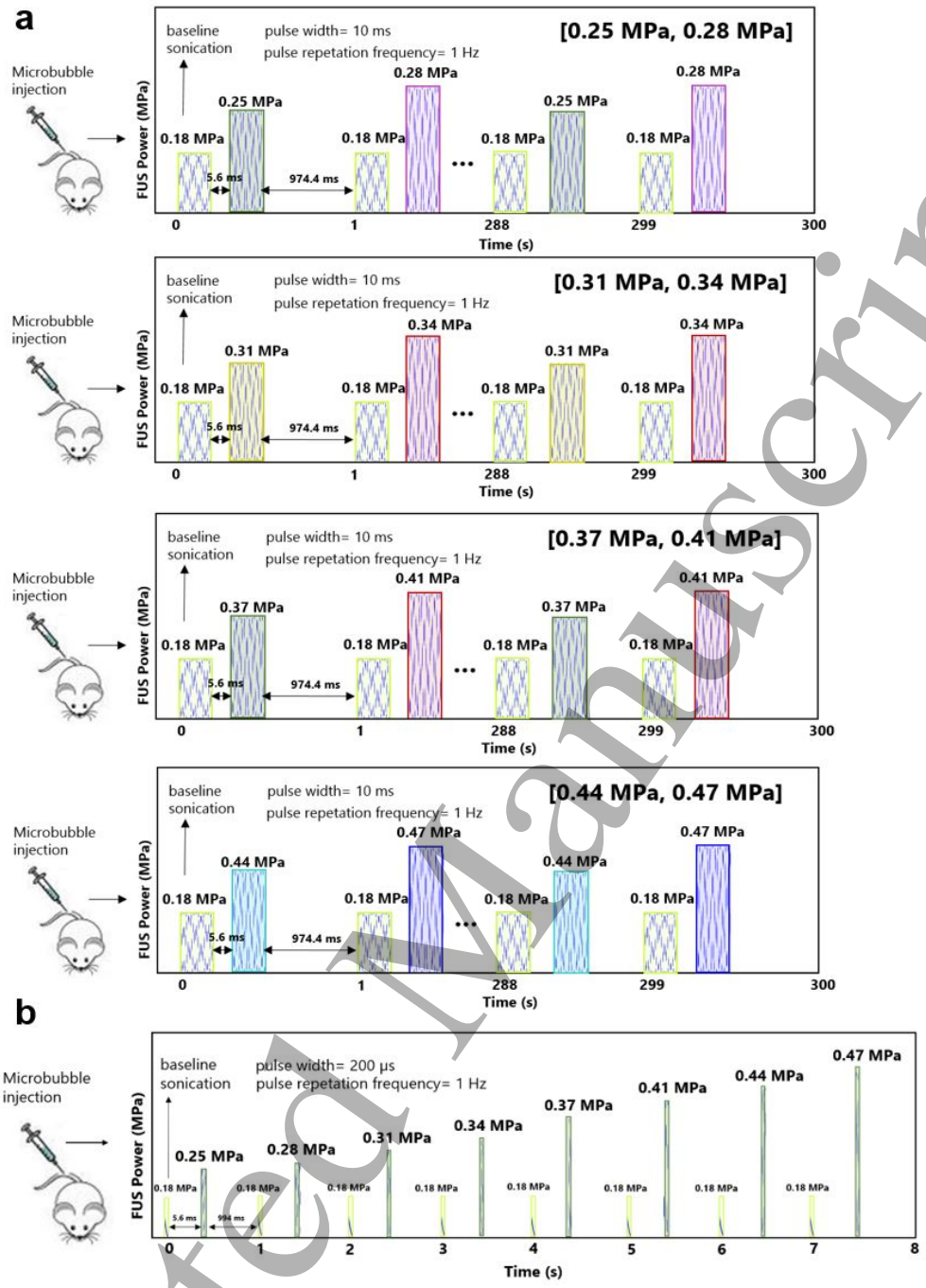

Figure 2. Sonication pulse sequences for long-term ICD monitoring and pre-calibration experiment. (a) Following 50 µL microbubble solution injection, FUS pulses at two different pressure levels are repeatedly applied (pulse duration=10 ms, PRF=1 Hz) for 5 min. A baseline pre-pulse of 0.18 MPa is applied 5.6 ms before the onset of each pulse in the sequence. The sonication sequence is repeated following a fresh MB injection to obtain the ICD curves for different FUS pressure pairs. The total duration of long-term ICD monitoring experiment to cover [0.25 MPa-0.47 MPa] range with 8 FUS pressure levels is 20 min excluding the duration of MB injection. **(b)** For pre-calibration experiments, short acoustic pulses (pulse duration=200 µs, PRF = 1 Hz) were applied to scan the same range of pressure levels as in the long-term ICD monitoring experiments. The total duration of pre-calibration ICD monitoring experiment to cover [0.25 MPa-0.47 MPa] range with 8 FUS pressure levels is 80 s for R=10 repetitions.

Sonication Experiments for Safety Analysis

To assess the safety and quantify the induced damage of the different cavitation bands, 7 mice were sonicated for each of the cavitation bands yielding a total of 28 animals. First, the pre-calibration experiment (0.25-0.62 MPa range, 1 min duration) was performed on each mouse to identify different cavitation regimes and to determine the boundaries of the operation band. Following the pre-calibration, 3-min sonication treatment was applied to each animal by using the feedback power control loop such that the instant ICD should fall into the desired cavitation zone. Furthermore, to validate the hypothesis that the short acoustic pulses applied during the pre-calibration experiment does not cause any considerable tissue damage, 7 mice were treated by only sonicating with the pre-calibration pulse trajectory as illustrated in Fig 2.b.

Histological Examination and Statistical Analysis

Whole brain histological analysis was performed on all brains. Animals were typically sacrificed 2 h after FUS exposure. The brain was transcardially perfused with 30 mL phosphate buffered saline (PBS) and 60 mL 4% paraformaldehyde. The post-fixation processing of the brain was then performed according to standard histological procedures. Serial horizontal cuts were performed every 250 μm starting from the surface of the brain and 10 sections were obtained for each brain. H&E staining was carried out in all sections to assess severity of hemorrhage, whilst BBB opening size was assessed on consecutive serial sections employing immunohistochemistry for albumin.

A hemorrhage-scoring scheme was used to quantify the severity of erythrocyte extravasation in each H&E-stained section. Separate scoring systems ranging from 0 to 3 were applied to assess the number of hemorrhages (0= no lesions; 1= < 5 hemorrhagic foci; 2= 6-20; and 3= > 20), the size of the hemorrhages (0= no lesions; 1= micro-hemorrhages, up to 30 μm in diameter; 2= small petechiae, up to 100 μm; and 3= large petechiae, often coalescing, composed of high numbers of erythrocytes, >100 μm in diameter) and the size of the affected area (0= no lesions; 1= the affected area is comprised within a 20 x power field, approx. 0.5 mm^2; 2= the affected area is comprised within a 10 x power field, approx. 2 mm^2, and 3 = the affected area is comprised within a 4x or lower power field (approx. equal or more than 12 mm^2). A final cumulative score for hemorrhage, ranging from (0) to (4), was obtained by summing the partial scores and was defined according to the following criteria: (1) Few,

focal small hemorrhages, (2) Few, multiple, moderately-sized hemorrhages or numerous multiple small hemorrhages, (3) Numerous, moderately sized or large, often coalescing hemorrhages, (4) Larger hemorrhages, often associated with significant vasogenic edema, characterized by vacuolation of the neuropil. Average final scoring for each animal was calculated summing the final scores for each section, excluding the first and the last. Figure.3 provides a graphical illustration of the proposed hemorrhage-scoring scheme. To determine whether the resulting hemorrhage scores were statistically different between the sonications operated at different cavitation bands, a one way ANOVA with Tukey post hoc analysis were deployed for pairwise comparisons where $p<0.01$ was considered to denote significant differences. The immunohistochemical staining for the albumin antigen served for the assessment of blood-brain barrier integrity (Saunders *et al.*, 2015). Immunohistochemistry was applied to four brain sections in each mouse, consecutive to those obtained for the H&E staining and taken at a distance of 1250 to 2000 μm from the dorsal surface of the brain. Briefly, sections were deparaffinized in xylene and rehydrated through graded ethanol. For antigen retrieval, sections were incubated in citrate buffer (pH 6.0) for 20 min at 98 °C. This was followed by incubation with a goat polyclonal albumin antibody (Bethyl A80-129A, 1:600 dilution in Dako antibody diluent, Dako-Agilent Technologies, Denmark) overnight at 4 °C. Afterwards, the slides were incubated for 30 min with a horseradish peroxidase (HRP)-labeled polymer, conjugated to a secondary anti-goat antibody (P0160, Dako-Agilent Technologies). The reaction was visualized using 3,3'-diaminobenzidine (DAB) as chromogen, followed by light counterstain with hematoxylin. The immunohistochemical staining was performed using an Autostainer (Dako Autostainer Universal Staining System Model LV-1, Dako-Agilent Technologies).

All immunolabeled slides were scanned using a digital slide scanner (NanoZoomer-XR C12000; Hamamatsu, Japan), and the area of albumin-positive regions was calculated in the digital slides using the Visiopharm Integrator System (VIS, version 4.5.1.324, Visiopharm, Hørsholm, Denmark). Briefly, a threshold classification allowed recognition of positive (brown) neuroparenchyma and negative regions.

Results

ICD kinetic curves and cavitation bands

A typical example for the kinetic curves obtained from Long-term ICD monitoring of a representative mouse is shown in Figure.4.a. It reveals a band structure formed by sudden jumps in ICD at certain pressure levels (0.37 MPa and 0.50 MPa) and related increase of the standard deviation. Also, there is a decrease in ICD over time particularly for the curves above the first jump point. We hypothesize: i) There exists an acoustic pressure dependent band structure of the long-term ICD curves with band-specific properties corresponding to different activity regimes. Different activitiy bands were identified based on the significant change in the magnitude of ICD curves such as steady oscillation band (SO), transition zone (TR), inertial cavitation band (IC) and high-pressure zone (HP). The bandwidth of each zone was defined by the standard deviation of the ICD data. ii) Although the driving acoustic pressure level is constant, ICD varies in time with a band-dependent standard deviation reflecting an intra-animal variation illustrated in Figure.4.c corresponding to the standard deviation of the ICD signals plotted in Figure 4.a. iii) The ICD levels defining the boundaries of different activity bands varies between individual animals revealing an inter-animal variation (Figure.4.b).

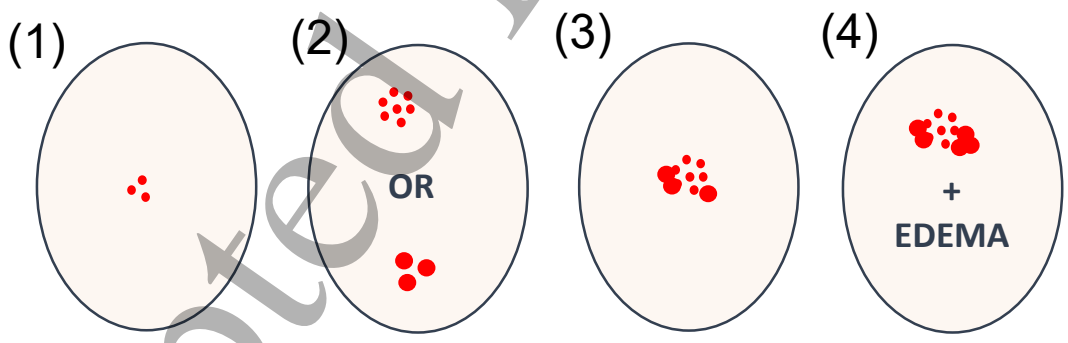

Figure 3. Hemorrhage scoring. The final hemorrhage-scoring scheme to quantify the severity of erythrocyte extravasation includes a score from 1-4 considering the number of hemorrhages, the size of hemorrhages, the size of affected area, the neuropil rarefaction. (1) Few, focal small hemorrhages (2) Few, multiple, moderately-sized hemorrhages or numerous multiple small hemorrhages (3) Numerous, moderately sized or large, often coalescing hemorrhage (4) Larger hemorrhages, often associated with significant vasogenic edema.

Pre-calibration experiments

Figure.5.a illustrates the long-term ICD kinetic curves of a specific animal and the identified activitiy zones. Figure.5.b shows the ICD curves and activitiy bands obtained from the pre-calibration experiment for the same animal. The qualitative comparison of the limits of the activitiy bands obtained from long-term monitoring and pre-calibration method implies that there is a good reproducibility between the two methods. For quantitative validation of the proposed pre-calibration method, the ICD values obtained from pre-calibration method *vs* long-term monitoring experiments were compared by calculating the correlation on seven animals that underwent in both experiments (Figure.5.c). While there is high correlation in the resulting ICD values obtained (R^2 = 0.81), the pre-calibration method takes much shorter time (N=8 pressures, R=10 repetitions, 8x10=80 s) relative to the long-term monitoring experiments (N=8 pressure levels, 8x5/2=20 min) and requires 4 fold less MB solution injection.

Closed-loop real-time feedback power control

Figure.6.a provides an overall summary of the developed closed-loop feedback power controller. The FUS pressure is initialized according to the desired operation band and increased with a discrete step-size of 1% of the maximum possible power corresponding to 0.03MPa acoustic pressure level (pulse duration 10 ms, PRF = 1 Hz). Figure.6.b illustrates how the applied FUS power is adaptively modulated to keep the instant ICD within the limits of the operation band. The control algorithm successfully assures a stable oscillation of the ICD within the desired operation band to induce the targeted cavitation activity. The physiological dissolution kinetics of the MBs led to an increasing pattern of the applied FUS exposure level to maintain the similar level of cavitation.

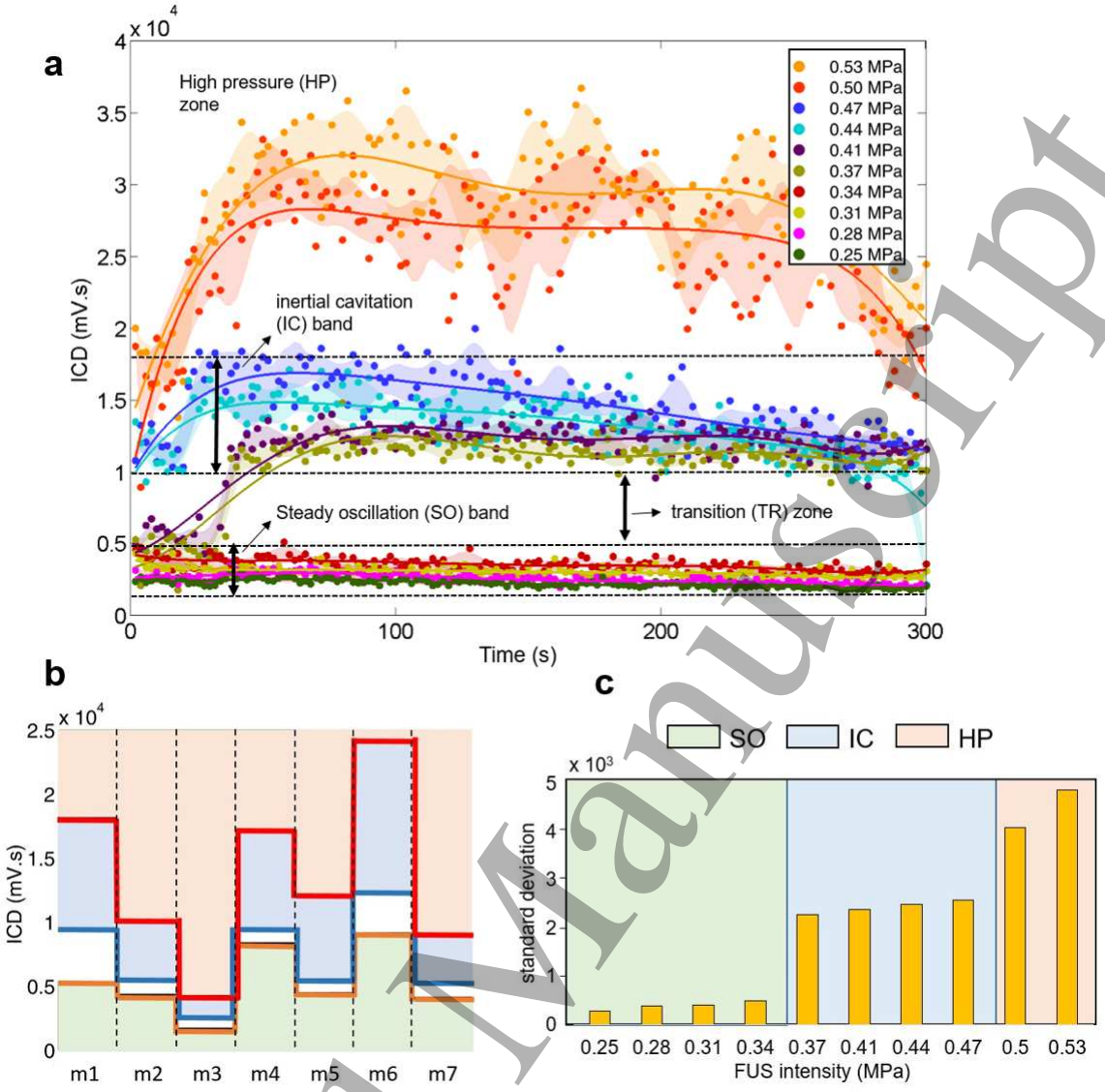

Figure 4. Long-term monitoring of ICD kinetic curves. (a) The long-term ICD kinetic curves were obtained from a representative mouse by executing the sonication pulse sequence illustrated in Figure 2. The long term monitoring duration to obtain all the ICD curves in the graph is 25 minutes (N=10 pressure levels) and the practical duration by considering the time for the preparation and injection of fresh MBs between sonications is approximately 25-30 min. There exists an acoustic pressure dependent band structure of the long-term ICD curves with band-specific properties corresponding to different activity regimes such as steady oscillation (SO) band, transition (TR) zone, inertial cavitation (IC) band and high-pressure (HP) zone. **(b)** The ICD levels defining the boundaries of specific activitiy bands vary between individual animals (5 min monitoring of each mouse from mouse 1 to mouse 7) revealing a setup-specific variations. **(c)** Although the driving acoustic pressure level is constant, ICD varies in time with a band-dependent standard deviation (standard deviation of the ICD curves if Fig.4.a.) reflecting characteristics of the respective activity mode.

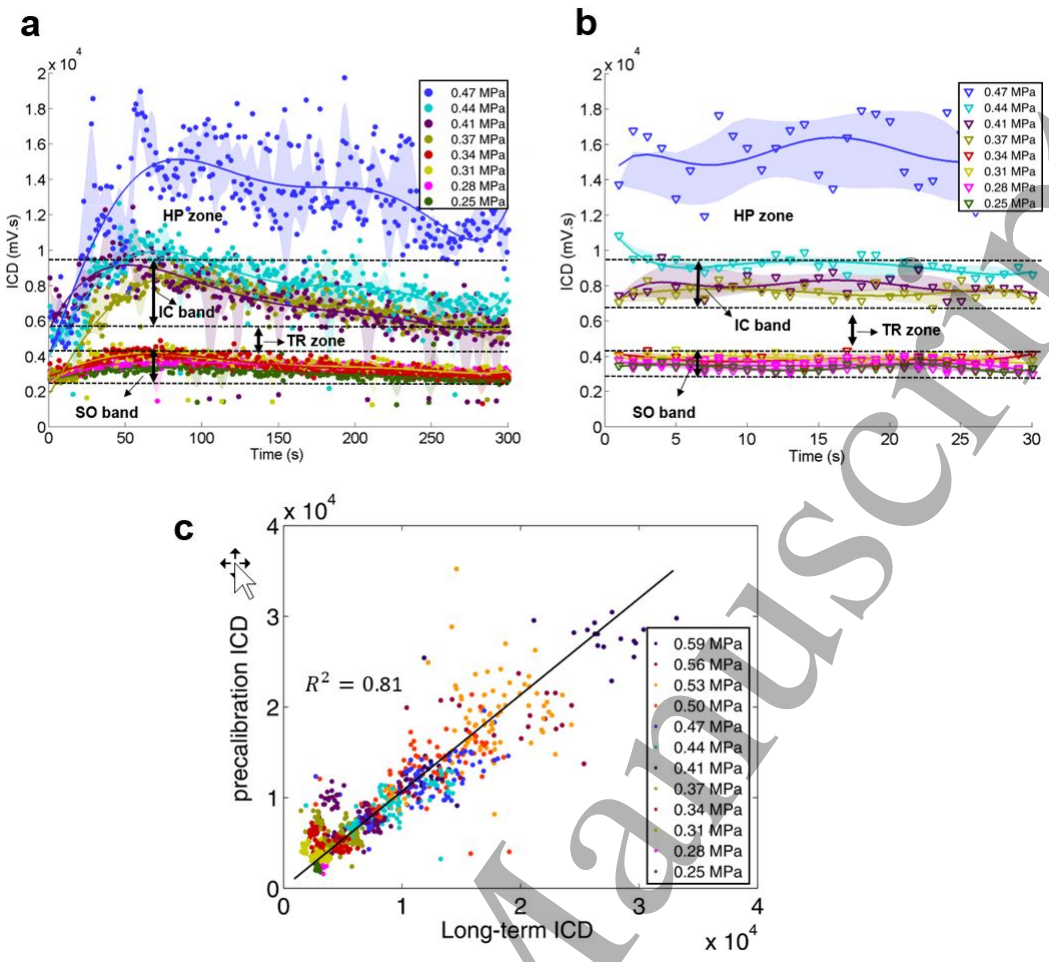

Figure 5. Pre-calibration method vs long-term ICD monitoring. (a) The long-term ICD kinetic curves of an individual animal. The total duration to obtain all the ICD curves in the graph is 20 min (N=8 pressure levels). Different cavitation activity regimes and zones such as steady oscillation (SO) band, transition (TR) zone, inertial cavitation (IC) band and high-pressure (HP) zone were identified based on the ICD kinetic curves **(b**) ICD curves and cavitation bands and zones obtained from the pre-calibration experiment for the same animal. The qualitative comparison of the limits of the transcranial cavitation bands obtained from long-term monitoring and pre-calibration method implies that there is a good reproducibility of the individual cavitation bands **(c)** Quantitative comparison of the ICD values for seven animals obtained from pre-calibration method and long-term ICD monitoring.

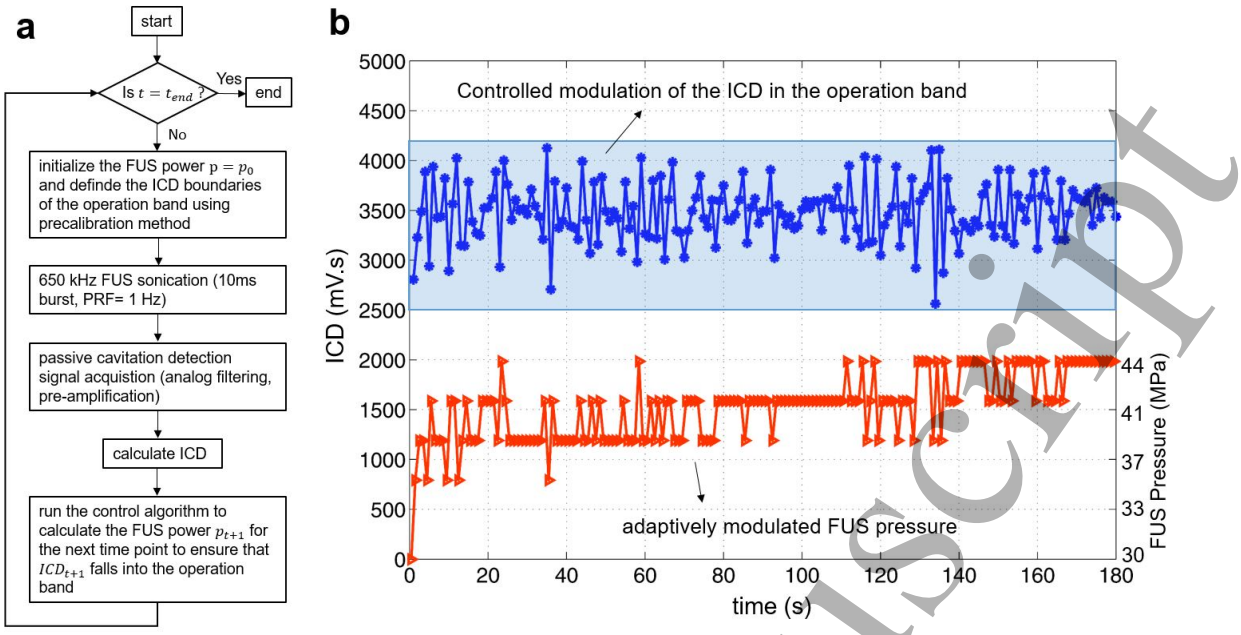

Figure 6. Closed-loop feedback power control. (a) Algorithmic scheme for the closed-loop feedback power control **(b)** The FUS power is dynamically updated to keep the instant ICD for the next time point should stay within the limits of the operation band.

BBB opening and safety

Following the successful execution of the FUS sonication such that the desired level of cavitation activity was induced, the severity of resulting tissue damage was assessed using histological examinations. The relation between the scale of erythrocyte extravasation measured by the proposed hemorrhage scoring scheme and the BBB opening volume obtained from the albumin immunohistochemistry for different exposure zones was monitored (Figure 7). Figure.7.a shows a representative photomicrograph of H&E-stained brain sections. An enhanced level of erythrocyte extravasation and neuroparenchymal hemorrhages with increasing cavitation activity was observed. Figure.7.b illustrates the BBB opening determined using albumin immunolabeling. There is a corresponding enlargement in the BBB opening size as a result of the increased cavitation activity. Figure.7.c demonstrates the severity of the tissue damage quantified using the proposed hemorrhage scoring scheme for different cavitation bands as a histogram plot (note that 7 animals were sonicated at each cavitation band). While average hemorrhage score is below (1) for pre-calibration experiments and SO band, it substantially increases with the increasing cavitation level. Correspondingly, there is a significant enlargement in the size of BBB opening with the enhanced cavitation activity provided by the histogram in Figure 7.d. The

statistically significant differences ($p<0.01$) for the hemorrhages scores and BBB opening size for different cavitation bands were indicated.

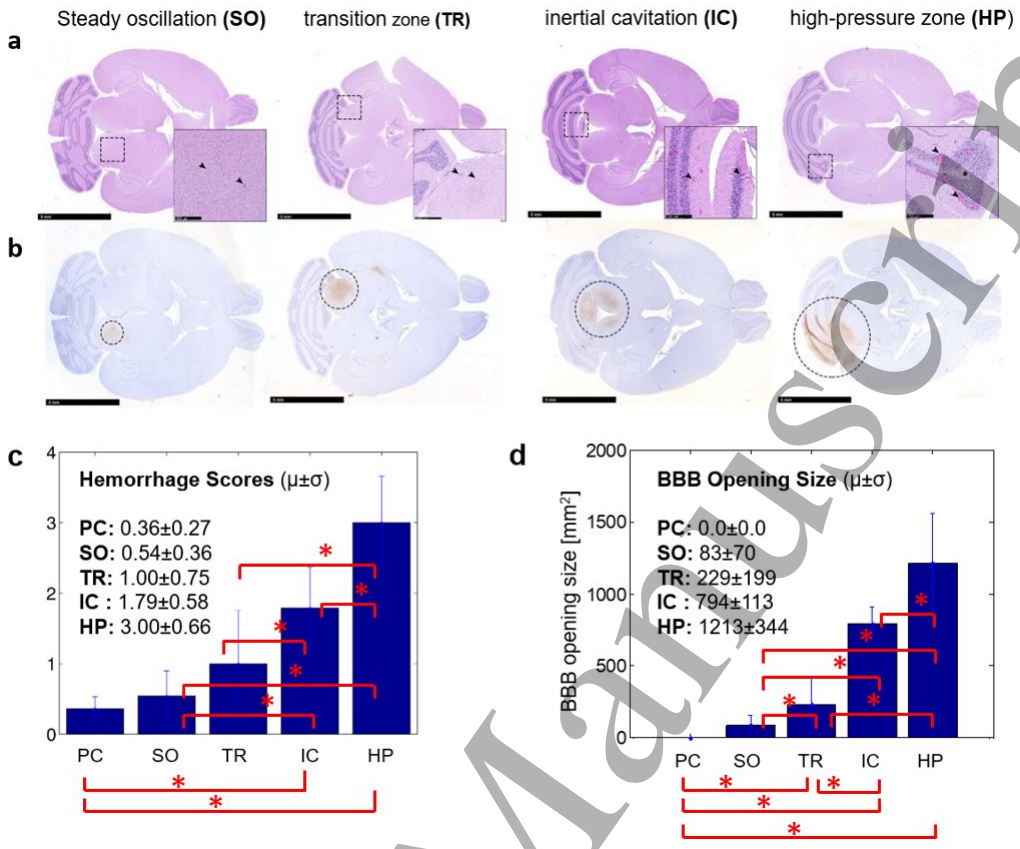

Figure 7. Activitiy band dependent safety characteristics and BBB opening size (a) Representative photomicrograph of H&E-stained brain sections exhibiting enhanced level of erythrocyte extravasation and neuroparenchymal hemorrhages with increasing cavitation activity (* denotes $p<0.01$) **(b)** enlargement in the BBB opening size with increasing cavitation activity determined using Albumin immunolabeling (* denotes $p<0.01$).

Discussion

In this study, we demonstrated a novel method to determine the in-situ, animal specific relationship between the acoustic pressure levels and induced cavitation activity to minimize the inter- and intra-animal effects during FUS therapy by using a specific type of long-circulating MBs (Schneider *et al.*, 2011) . Note that the boundaries of the specific activity regimes are highly dependent to the physical (i.e. experimental setup, geometry, acoustic coupling) and physiological (i.e. inter-animal variation, physiological condition) dynamics of the experiment. The major advantage of the proposed method is that it enables to characterize different level of activities with corresponding 'activity bands' for an individual animal and for the given experimental

conditions in a short amount of time and without causing any macro tissue damage. Determining the boundaries of the cavitation doses for different cavitation regimes allows to run the FUS treatment at a selected operation band to suppress the occurrence of IC with the ultimate goal of maximizing the BBB opening while avoiding macro tissue damage. Furthermore, in order to stably execute the FUS sonication in the pre-determined operation band and account for the variations in bubble kinetics and physiological conditions of the animal, we developed and validated a closed-loop, real-time transcranial cavitation control framework. With the controller, we were able to optimize the FUS pressure instantly and modulate it in real-time to maintain the targeted cavitation level for the time course of the treatment while improving safety control.

In previous studies, the correlation between spectral components of the MB emission and FUS induced BBB opening have been reported in different animal models (Wu *et al.*, 2016; Vykhodtseva *et al.*, 1995). It has been shown that harmonic, sub-harmonic, ultra-harmonic activity and broad-band noise can serve as indicators to measure the cavitation level and therefore to monitor BBB opening (McDannold *et al.*, 2006; Tung *et al.*, 2010a). In the present work, the broadband response as detected by PCD was quantified using the ICD. This was based on previous approaches that reported significant correlation between the broadband noise and inertial cavitation (Tung *et al.*, 2010b). Note that relatively poor vertical resolution of the digitizer used in this study (8 bits) the limited frequency bandwidth of the PCD transducer could affect the ICD quantification. In this respect, filtering the 1st and 2nd harmonic of the PCD signal could help in decreasing the dynamic range of the signal. However, windowing reduces the energy of the signal and also blur the energy at specific frequencies over nearby frequencies (Haworth *et al.*, 2017). Compensating for such a convoluted representation can be difficult and encoding the signal with a high resolution hardware is preferable.

The results obtained by using long circulating MBs lead to understanding the long-term temporal dynamics of the cavitation activity measured by ICD. The sudden jump in the ICD curves above a certain pressure level is actually in agreement with the results reported by (Tung *et al.*, 2010b) where it was found that the ICD at 0.45 MPa and 0.60 MPa was statistically higher than that of 0.30 and 0.15 MPa indicating a threshold for inertial cavitation and BBB opening. The ICD curves below the first jump pressure

represents a SO activity or composes a ‘steady oscillation regime’ while those above the jump pressure represent IC or create an ‘inertial cavitation regime’ following a ‘transition zone’. Further increase in the acoustic pressure causes a second jump that could be defined as a separate ‘high pressure zone’. The increased standard deviation in higher operation bands might be linked to both physical and physiological sources. On the physical side, the mechanistic response of the oscillating MBs under an acoustic field could be more unsteady and variable at high-pressure levels relative to low-pressure levels. This might be reflected in the ICD curves at ‘inertial cavitation regime’ as an increased standard deviation in time. Furthermore, the physiological condition of the sonicated animal might also significantly change during the course of the experiment as a response to increased applied acoustic pressure to the brain. This might also contribute to the increased standard deviation of the ICD values at higher-pressure levels. Finally, the decreasing tendency of the ICD values over time is probably due to the decreased bubble quality and concentration because of distortion and collapse under the acoustic field and blood circulation.

The outcomes of the long term ICD monitoring regarding the inter-animal variations imply that it is hard to define a global ICD threshold for a certain cavitation regime that is valid for all animals and independent from all deployed experimental geometry and setup and its coupling between the animal. In principle, long-term ICD kinetic curves of a specific animal may serve as a gold standard to determine the boundaries of the cavitation regimes to run the experiment within a specific operation band depending on the demands of the experiment such as occurrence and size of the BBB opening. However, there are some major challenges in such an approach: First, the full long-term monitoring of the ICD kinetics may take around 20-30 min depending on the range of scanned pressure levels that is certainly not feasible in experiments. Second, it is required to inject a certain amount of MB suspension to obtain the long-term ICD kinetic curves that limits the amount of applicable liquid for the rest of the experiments. Third, monitoring the ICD curves particularly for higher pressure levels are subject to safety concerns. Therefore, the proposed pre-calibration method substantially speeds-up the process to safely determine animal-specific transcranial cavitation thresholds for the targeted cavitation regime with minimum possible liquid injection. This finding is promising because it suggests physically and physiologically independent cavitation thresholds.

A further concern is subject to safety and the proposed pre-calibration method relies on the assumption that short FUS pulses (200 μs duration) in the prescribed pressure range do not cause any macro tissue damage. To validate the proposed approach for the safety concerns, a separate set of experiment was designed and performed on seven mice where the animals went through pre-calibration experiment only. The resulting average hemorrhage scoring (0.36 ± 0.47) implies that pre-calibration method does not cause any considerable red-blood cell extravasation and is fully safe for executing before the actual sonication treatment to determine the in-situ, animal specific transcranial cavitation limits.

To stably run the experiment within the determined operation band, a closed-loop adaptive feedback power controller was developed. The major challenge for the control problem is the time-varying MB kinetics and animal physiology. In the pilot experiments for deciding the optimum FUS pressure level that will be applied at the next time point, it has been observed that taking into account a certain history instead of using the recent ICD value increases the stabilization of ICD controlling challenge. In order to improve the control over the instant cavitation level, the controller algorithm allows to select the size of the window in which the previous ICD values are included. Our findings indicate that assessing a longer ICD history more than 10 s did not created a considerable change in the next FUS pressure level.

The histological findings in this work are consistent with the existing literature that explored the correlation between inertial cavitation and erythrocyte extravasation (Hwang *et al.*, 2006; Samuel *et al.*, 2009; Tung *et al.*, 2010b; Tsai *et al.*, 2016). It has been previously reported that excessive FUS exposure may result varying severity of erythrocyte extravasation which might be minor without causing any hazard or large scale inducing significant vascular and neuronal damage (Hynynen *et al.*, 2005; Liu *et al.*, 2008). In general, it is well-accepted that strong IC could increase the likelihood of the damage and enhances the post-safety concerns. In this study, we additionally explored the BBB opening size achieved at different activity bands and corresponding safety characteristics of each band quantitatively measured by a proposed hemorrhage scoring scheme. The high correlation ($r^2 = 0.84$) between the band dependent BBB opening size and the hemorrhage scores indicate that there is a tradeoff between efficiency and safety. Operating the experiment at SO band or in the transition zone results a relatively lower average hemorrhage score suggesting a safe sonication without any considerable damage. While the BBB opening size becomes

larger for the IC band and high-pressure zone as expected, the resulting hemorrhage scores are not acceptable for the operation.

Contrast enhanced magnetic resonance imaging (MRI) or T_2^* weighted imaging could alternatively be used for assessing the size of BBB opening and damage (Hynynen *et al.*, 2001; McDannold *et al.*, 2012; Marquet *et al.*, 2011). However, MRI-based safety assessment has to be performed after the sonication and the long pulse sequence duration needed to acquire the image makes it highly challenging to integrate with a closed-loop feedback control framework. Moreover, vascular damage could take much longer (tens of seconds) to appear in MRI that further limits its usage as a real time control system.

While the described closed-loop cavitation control methods have been applied successfully in a preclinical study in mouse models of Glioblastoma Multiforme to deliver 80nm-sized liposomal MGMT inactivators (Signorell *et al.*, 2018) to reverse chemoresistance against temozolomide (Papachristodoulou et al., 2018), several factors could improve the presented work. First, to extend the proposed methods for potential clinical use, the effect of many different factors has to be investigated mainly including the spatial attenuation due to the skull (Tung *et al.*, 2010a) where the increased distance to the focal point will decrease the detection sensitivity of the cavitation signal. Second, it has been reported that the heterogeneity of the brain anatomy and vasculature (presence of large cerebral vessels, gray and white matter) significantly affects the cavitation activity (Wu *et al.*, 2016) mainly because the MBs circulating in large vessels exhibits a different response to FUS exposure (Sassaroli and Hynynen, 2006, 2007). Therefore, it would also be beneficial to study the effect of the tissue type on the strength of the cavitation signal and the ultimate controller behavior for future studies. The clinical translation of the presented method certainly needs scaling to larger animal models because the presence of the skull is a major challenge for the application of the FUS-mediated BBB opening. It has been recently demonstrated a feed-back control system for ultrasound mediated BBB disruption with high-field MRI guidance in monkeys (Kamimura *et al.*, 2018). The proposed pre-calibration method in this work could be integrated in such a framework to improve the efficacy and safety of the treatments by minimizing the inter- and intra-animal variability and the effects of *in-situ* experimental conditions. Moreover, the infusion rate of the MBs can be optimized such that it compensates the decreasing tendency of the bubble kinetics and provides a cavitation signal in steady-state for the constant pressure

levels. To achieve this, future work could consider the infusion rate as an additional constraint in the optimization problem of the control algorithm. Finally, in this study, passive cavitation detection was performed using a single channel receiver that collects all the emission signal from the active field. Passive cavitation imaging to achieve a spatially resolved cavitation activity map (Arvanitis *et al.*, 2013; O'Reilly *et al.*, 2014; Gateau *et al.*, 2011) or binary cavitation localization using a single PCD (Maimbourg *et al.*, 2018) may be integrated to the proposed controller framework to improve its performance.

Acknowledgements

This work was supported by a Sinergia grant from the Swiss National Science Foundation (SNSF, CRSII3_147651 to J.C.L., E.M. and M.W.). We thank Bracco Suisse SA, Geneva for providing microbubbles and valuable discussions, and Markus Marks from from Neurotechnology Group at ETH Zurich for technical support.

Appendix

By assuming a constant scalar relation between the applied FUS power (p) and the resulting ICD level (ICD) in a simplified case such that

$$ICD_t = c.p_t$$
$$ICD_{t-1} = c.p_{t-1}$$
$$\dots$$
$$ICD_{t-k} = c.p_{t-k}$$

where t is time and k is the number of samples that have an effect on the ICD level for $(k+1)$ $^{\text{th}}$ sample. In other words k is the window size that is assessed as the history to determine for the next time point's FUS power. If the ideal ICD level to operate the treatment is ICD_{id} (i.e. mean of the operation band), than the cost function is defined as

$$\min_c \sum_{i=0}^{k} (ICD_{id} - ICD_{t-i})^2 \qquad [1]$$

If the Eq.1 is solved for c,

$$\frac{\partial}{\partial c}\left(\min_{c}\sum_{i=0}^{k}(ICD_{id}-c.p_{t-i})^2\right)=0 \quad [2]$$

$$c=\frac{\sum_{i=0}^{k}ICD_{id}.p_{t-i}}{\sum_{i=0}^{k}p_{t-i}^2} \quad [3]$$

Then the power level that has to be applied for the time point $(t+1)$ is given as

$$p_{t+1}=\frac{ICD_{id}}{c} \quad [4]$$

By considering a more realistic case where the applied FUS power (p) does not only has a constant scalar relation with ICD level (ICD) but a linear relationship such that

$$ICD_t = c_1.p_t + c_2.p_{t-1} + \cdots + c_k.p_{t-(k-1)} \quad [5]$$

Then ICD_{t+1} will be

$$ICD_{t+1} = c_1.p_{t+1} + c_2.p_t + \cdots + c_k.p_{(t-k)} \quad [6]$$

Let us define A as

$$A = c_2.p_t + \cdots + c_k.p_{(t-k)} \quad [7]$$

Then,

$$ICD_{t+1} = c_1.p_{t+1} + A \quad [8]$$

$$p_{t+1}=\frac{ICD_{t+1}-A}{c_1} \quad [9]$$

The equations can be written in matrix form such that **X** is a kxk matrix (2k window size) and **ICD** is kx1 vector such as

$$\mathbf{X} = \begin{bmatrix} p_t & p_{t-1} & \cdots & p_{t-k} \\ \vdots & & \ddots & \vdots \\ p_{t-k} & p_{t-k-1} & \cdots & p_{t-2k} \end{bmatrix} \quad [10]$$

$$\mathbf{ICD} = [ICD_t \; ICD_{t-1} \ldots ICD_{t-k}]^T \quad [11]$$

$$\mathbf{w} = [c_1, c_2, \ldots, c_k] \quad [12]$$

Then, the coefficients are calculated with the following closed form solution such as

$$\mathbf{w} = (\mathbf{X}^T\mathbf{X})^{-1}\mathbf{X}^T\mathbf{ICD} \quad [13]$$

After computing the coefficients $\mathbf{w}$, one can calculate A and substitute in Eq.9 to find out the p_{t+1}.

References

Arvanitis C D, Livingstone M S and McDannold N 2013 Combined ultrasound and MR imaging to guide focused ultrasound therapies in the brain *Phys Med Biol* **58** 4749-61

Arvanitis C D, Livingstone M S, Vykhodtseva N and McDannold N 2012 Controlled Ultrasound-Induced Blood-Brain Barrier Disruption Using Passive Acoustic Emissions Monitoring *Plos One* **7**

Aryal M, Arvanitis C D, Alexander P M and McDannold N 2014 Ultrasound-mediated blood-brain barrier disruption for targeted drug delivery in the central nervous system *Advanced Drug Delivery Reviews* **72** 94-109

Baseri B, Choi J J, Deffieux T, Samiotaki G, Tung Y S, Olumolade O, Small S A, Morrison B and Konofagou E E 2012 Activation of signaling pathways following localized delivery of systemically administered neurotrophic factors across the blood-brain barrier using focused ultrasound and microbubbles *Phys Med Biol* **57** N65-N81

Carpentier A, Canney M, Vignot A, Reina V, Beccaria K, Horodyckid C, Karachi C, Leclercq D, Lafon C, Chapelon J Y, Capelle L, Cornu P, Sanson M, Hoang-Xuan K, Delattre J Y and Idbaih A 2016 Clinical trial of blood-brain barrier disruption by pulsed ultrasound *Science Translational Medicine* **8**

Chen H and Konofagou E E 2014 The size of blood-brain barrier opening induced by focused ultrasound is dictated by the acoustic pressure *Journal of Cerebral Blood Flow and Metabolism* **34** 1197-204

Choi J J, Wang S G, Tung Y S, Morrison B and Konofagou E E 2010 Molecules of Various Pharmacologically-Relevant Sizes Can Cross the Ultrasound-Induced Blood-Brain Barrier Opening in Vivo *Ultrasound Med Biol* **36** 58-67

Gateau J, Aubry J F, Pernot M, Fink M and Tanter M 2011 Combined Passive Detection and Ultrafast Active Imaging of Cavitation Events Induced by Short Pulses of High-Intensity Ultrasound *Ieee T Ultrason Ferr* **58** 517-32

Haworth K J, Bader K B, Rich K T, Holland C K and Mast T D 2017 Quantitative Frequency-Domain Passive Cavitation Imaging *Ieee T Ultrason Ferr* **64** 177-91

Hwang J H, Tu J, Brayman A A, Matula T J and Crum L A 2006 Correlation between inertial cavitation dose and endothelial cell damage in vivo *Ultrasound Med Biol* **32** 1611-9

Hynynen K, McDannold N, Sheikov N A, Jolesz F A and Vykhodtseva N 2005 Local and reversible blood-brain barrier disruption by noninvasive focused ultrasound at frequencies suitable for trans-skull sonications *Neuroimage* **24** 12-20

Hynynen K, McDannold N, Vykhodtseva N and Jolesz F A 2001 Noninvasive MR imaging-guided focal opening of the blood-brain barrier in rabbits *Radiology* **220** 640-6

Jordao J F, Thevenot E, Markham-Coultes K, Scarcelli T, Weng Y Q, Xhima K, O'Reilly M, Huang Y X, McLaurin J, Hynynen K and Aubert I 2013 Amyloid-beta plaque reduction, endogenous antibody delivery and glial activation by brain-targeted, transcranial focused ultrasound *Experimental Neurology* **248** 16-29

Kamimura H, Flament J, Valette J, Cafarelli A, Badin R, Hantraye P and Larrat B 2018 Feedback control of microbubble cavitation for ultrasound-mediated blood-brain barrier disruption in non-human primates under magnetic resonance guidance *Journal of Cerebral Blood Flow and Metabolism*

Kovacs Z, Werner B, Rassi A, Sass J O, Martin-Fiori E and Bernasconi M 2014 Prolonged survival upon ultrasound-enhanced doxorubicin delivery in two syngenic glioblastoma mouse models (vol 187, pg 74, 2014) *Journal of Controlled Release* **192** 294-

Lipsman N, Meng Y, Bethune A J, Huang Y X, Lam B, Masellis M, Herrmann N, Heyn C, Aubert I, Boutet A, Smith G S, Hynynen K and Black S E 2018 Blood-brain barrier opening in Alzheimer's disease using MR-guided focused ultrasound *Nat Commun* **9**

Liu H L, Hua M Y, Chen P Y, Chu P C, Pan C H, Yang H W, Huang C Y, Wang J J, Yen T C and Wei K C 2010 Blood-Brain Barrier Disruption with Focused Ultrasound Enhances Delivery of Chemotherapeutic Drugs for Glioblastoma Treatment *Radiology* **255** 415-25

Liu H L, Wai Y Y, Chen W S, Chen J C, Hsu P H, Wu X Y, Huang W C, Yen T C and Wang J J 2008 Hemorrhage detection during focused-ultrasound induced blood-brain-barrier opening by using susceptibility-weighted magnetic resonance imaging *Ultrasound Med Biol* **34** 598-606

Magnin R R F, Salabartan F, Meriaux S, Aubry JF, Bihan D, Dumont E, Larrat B 2015 Magnetic resonance-guided motorized transcranial ultrasound system for blood-brain barrir permeabilization along arbitrary trajectories in rodents *Journal of therapeutic ultrasound* **3**

Maimbourg G, Houdouin A, Santin M, Lehericy S, Tanter M and Aubry J F 2018 Inside/outside the brain binary cavitation localization based on the lowpass filter effect of the skull on the harmonic content: a proof of concept study *Phys Med Biol* **63**

Marquet F, Tung Y S, Teichert T, Ferrera V P and Konofagou E E 2011 Noninvasive, Transient and Selective Blood-Brain Barrier Opening in Non-Human Primates In Vivo *Plos One* **6**

Marty B, Larrat B, Van Landeghern M, Robic C, Robert P, Port M, Le Bihan D, Pernot M, Tanter M, Lethimonnier F and Meriaux S 2012 Dynamic study of blood-brain barrier closure after its disruption using ultrasound: a quantitative analysis *Journal of Cerebral Blood Flow and Metabolism* **32** 1948-58

McDannold N, Arvanitis C D, Vykhodtseva N and Livingstone M S 2012 Temporary Disruption of the Blood-Brain Barrier by Use of Ultrasound and Microbubbles: Safety and Efficacy Evaluation in Rhesus Macaques *Cancer Research* **72** 3652-63

McDannold N, Vykhodtseva N and Hynynen K 2006 Targeted disruption of the blood-brain barrier with focused ultrasound: association with cavitation activity *Phys Med Biol* **51** 793-807

McDannold N, Vykhodtseva N, Raymond S, Jolesz F A and Hynynen K 2005 MRI-guided targeted blood-brain barrier disruption with focused ultrasound: Histological findings in rabbits *Ultrasound Med Biol* **31** 1527-37

Miller M W, Miller D L and Brayman A A 1996 A review of in vitro bioeffects of inertial ultrasonic cavitation from a mechanistic perspective *Ultrasound Med Biol* **22** 1131-54

Neppiras E A 1984 Acoustic Cavitation Series .1. Acoustic Cavitation - an Introduction *Ultrasonics* **22** 25-8

O'Reilly M A and Hynynen K 2012 Blood-Brain Barrier: Real-time Feedback-controlled Focused Ultrasound Disruption by Using an Acoustic Emissions-based Controller *Radiology* **263** 96-106

O'Reilly M A, Jones R M and Hynynen K 2014 Three-Dimensional Transcranial Ultrasound Imaging of Microbubble Clouds Using a Sparse Hemispherical Array *Ieee T Bio-Med Eng* **61** 1285-94

Pouliopoulos A N, Bonaccorsi S and Choi J J 2014 Exploiting flow to control the in vitro spatiotemporal distribution of microbubble-seeded acoustic cavitation activity in ultrasound therapy *Phys Med Biol* **59** 6941-57

Pouliopoulos A N, Li C Q, Tinguely M, Garbin V, Tang M X and Choi J J 2016 Rapid short-pulse sequences enhance the spatiotemporal uniformity of acoustically driven microbubble activity during flow conditions *J Acoust Soc Am* **140** 2469-80

Samuel S, Fowlkes J B and Miller D L 2009 An In Vitro Study of the Correlation Between Bubble Distribution, Acoustic Emission, and Cell Damage by Contrast Ultrasound *Ieee T Ultrason Ferr* **56** 589-99

Sassaroli E and Hynynen K 2006 On the impact of vessel size on the threshold of bubble collapse *Appl Phys Lett* **89**

Sassaroli E and Hynynen K 2007 Cavitation threshold of microbubbles in gel tunnels by focused ultrasound *Ultrasound Med Biol* **33** 1651-60

Saunders N R, Dziegielewska K M, Mollgard K and Habgood M D 2015 Markers for blood-brain barrier integrity: how appropriate is Evans blue in the twenty-first century and what are the alternatives? *Front Neurosci-Switz* **9**

Schneider M, Anantharam B, Arditi M, Bokor D, Broillet A, Bussat P, Fouillet X, Frinking P, Tardy I, Terrettaz J, Senior R and Tranquart F 2011 BR38, a New Ultrasound Blood Pool Agent *Investigative Radiology* **46** 486-94

Signorell R D, Papachristodoulou A, Xiao J, Arpagaus B, Casalini T, Grandjean J, Thamm J, Steiniger F, Luciani P, Brambilla D, Werner B, Martin E, Weller M, Roth P and Leroux J C 2018 Preparation of PEGylated liposomes incorporating lipophilic lomeguatrib derivatives for the sensitization of chemo-resistant gliomas *Int J Pharmaceut* **536** 388-96

Sun T, Samiotaki G, Wang S, Acosta C, Chen C C and Konofagou E E 2015 Acoustic cavitation-based monitoring of the reversibility and permeability of ultrasound-induced blood-brain barrier opening *Phys Med Biol* **60** 9079-94

Sun T, Zhang Y Z, Power C, Alexander P M, Sutton J T, Aryal M, Vykhodtseva N, Miller E L and McDannold N J 2017 Closed-loop control of targeted ultrasound drug delivery across the blood-brain/tumor barriers in a rat glioma model *P Natl Acad Sci USA* **114** E10281-E90

Timbie K F, Mead B P and Price R J 2015 Drug and gene delivery across the blood-brain barrier with focused ultrasound *Journal of Controlled Release* **219** 61-75

Treat L H, McDannold N, Zhang Y Z, Vykhodtseva N and Hynynen K 2012 Improved Anti-Tumor Effect of Liposomal Doxorubicin after Targeted Blood-Brain Barrier Disruption by Mri-Guided Focused Ultrasound in Rat Glioma *Ultrasound Med Biol* **38** 1716-25

Tsai C H, Zhang J W, Liao Y Y and Liu H L 2016 Real-time monitoring of focused ultrasound blood-brain barrier opening via subharmonic acoustic emission detection: implementation of confocal dual-frequency piezoelectric transducers *Phys Med Biol* **61** 2926-46

Tung Y S, Choi J J, Baseri B and Konofagou E E 2010a Identifying the Inertial Cavitation Threshold and Skull Effects in a Vessel Phantom Using Focused Ultrasound and Microbubbles *Ultrasound Med Biol* **36** 840-52

Tung Y S, Vlachos F, Choi J J, Deffieux T, Selert K and Konofagou E E 2010b In vivo transcranial cavitation threshold detection during ultrasound-induced blood-brain barrier opening in mice *Phys Med Biol* **55** 6141-55

Tung Y S, Vlachos F, Feshitan J A, Borden M A and Konofagou E E 2011 The mechanism of interaction between focused ultrasound and microbubbles in blood-brain barrier opening in mice *J Acoust Soc Am* **130** 3059-67

Vykhodtseva N I, Hynynen K and Damianou C 1995 Histologic Effects of High-Intensity Pulsed Ultrasound Exposure with Subharmonic Emission in Rabbit Brain in-Vivo *Ultrasound Med Biol* **21** 969-79

Wu S Y, Sanchez C S, Samiotaki G, Buch A, Ferrera V P and Konofagou E E 2016 Characterizing Focused-Ultrasound Mediated Drug Delivery to the Heterogeneous Primate Brain In Vivo with Acoustic Monitoring *Scientific Reports* **6**

Wu S Y, Tung Y S, Marquet F, Downs M E, Sanchez C S, Chen C C, Ferrera V and Konofagou E 2014 Transcranial Cavitation Detection in Primates During Blood-Brain Barrier Opening-A Performance Assessment Study *Ieee T Ultrason Ferr* **61** 966-78